# Modeling the dynamical friction timescale of a sinking satellite *

Jian-Ling Gan[1,3], Xi Kang[2], Jin-Liang Hou[1] and Rui-Xiang Chang[1]

[1]  Key Laboratory for Research in Galaxies and Cosmology, Shanghai Astronomical Observatory,
   Chinese Academy of Sciences, Shanghai 200030, China; *jlgan@shao.ac.cn*
[2]  Purple Mountain Observatory, Chinese Academy of Sciences, Nanjing 210008, China
[3]  Graduate University of Chinese Academy of Sciences, Beijing 100049, China

**Abstract**  When a satellite galaxy falls into a massive dark matter halo, it suffers
from the dynamical friction force which drags it into the halo's center, where it finally
merges with the central galaxy. The time interval between entry and merger is called
the dynamical friction timescale ($T_{\mathrm{df}}$). Many studies have been dedicated to deriving
$T_{\mathrm{df}}$ using analytical models or $N$-body simulations. These studies have obtained qual-
itative agreements on how $T_{\mathrm{df}}$ depends on the orbital parameters, and the mass ratio
between the satellite and the host's halo. However, there are still disagreements on
deriving an accurate form for $T_{\mathrm{df}}$. We present a semi-analytical model to predict $T_{\mathrm{df}}$
and we focus on interpreting the discrepancies among different studies. We find that
the treatment of mass loss from the satellite by tidal stripping dominates the behavior
of $T_{\mathrm{df}}$. We also identify other model parameters which affect the predicted $T_{\mathrm{df}}$.

**Key words:**  methods: analytical — methods: numerical — galaxies: haloes — galax-
ies: evolution — galaxies: interactions — cosmology: dark matter

## 1 INTRODUCTION

In the standard cold dark matter (CDM) model, galactic structures (dark matter halos) grow in a
hierarchical manner. During the merger of two dark matter halos, the less massive one becomes
the satellite[1] (or subhalo) of the more massive one (host halo). The satellite will orbit the host and
finally merge with the host halo. Halo mergers play an important role in the formation and evolution
of galaxies, as they can significantly affect the star formation rate, color and morphology of galaxies
(e.g., Benson et al. 2002, 2004; Kang et al. 2005; Kazantzidis et al. 2008). Therefore, one inevitable
question about galaxy formation and evolution in the CDM scenario is to find out how long it takes
for the satellite to merge with the host halo.

   Dynamical friction is the primary mechanism which decreases the orbital energy and angular
momentum of a satellite, and drags it into the host halo's center. A description of dynamical friction
was first given by Chandrasekhar  (1943), who derived a formula for dynamical friction based on
the idealized case that a rigid body moves through an infinite, homogeneous sea of field particles.

---

[1]  When we refer to a satellite, we mean the dark matter subhalo, not its luminous counterpart which is often called a
satellite galaxy.

In most cases, the satellite is moving through a finite host halo, and the dynamical friction timescale ($T_{\mathrm{df}}$) of the satellite is defined as the time interval between entry and merger with the host's center. A simple application of Chandrasekhar's formula to derive $T_{\mathrm{df}}$ for a rigid satellite is given by Binney & Tremaine (1987, hereafter BT87) and Lacey & Cole (1993, hereafter LC93), and these formulas are widely used in semi-analytical models of galaxy formation and evolution (e.g., Kauffmann et al. 1999; Cole et al. 2000; Somerville & Primack 1999; Neistein & Weinmann 2010). The early study of Navarro et al. (1995) found that the LC93 formula could accurately match their simulation results. However, the simulation results of Springel et al. (2001) and Kang et al. (2005) indicated that the LC93 formula underestimates the merging timescale and overestimates the merger rate since LC93 is only valid for a rigid object, not for an amorphous satellite in simulations.

For an amorphous satellite, one needs to take into account the effect of tidal force, which leads to mass loss from the satellite and redistribution of mass inside of it. Deriving an analytical formula of $T_{\mathrm{df}}$ for a real satellite is nontrivial as one has to follow both the orbit and mass evolution. Colpi et al. (1999, hereafter C99) first questioned the conclusion of Navarro et al. (1995), and they found that tidal stripping can significantly increase $T_{\mathrm{df}}$. This conclusion was recently confirmed by Boylan-Kolchin et al. (2008, hereafter BK08) and Jiang et al. (2008, hereafter J08) using high resolution simulations. BK08 and J08 both gave fitting formulas for $T_{\mathrm{df}}$, but with different dependences on orbital parameters. Their results differ by a factor of up to two for eccentric orbits. Using a semi-analytical model with the inclusion of tidal effects, Taffoni et al. (2003, hereafter T03) derived a fitting formula for $T_{\mathrm{df}}$. However, their results are not well tested in simulations. Moreover, the prediction of T03 is quantitatively inconsistent with the results of BK08 and J08.

In this paper, we use a semi-analytical model to study $T_{\mathrm{df}}$ of a satellite. Our main motivation is neither to get a consistent result with simulations or other models, nor to derive a reasonable $T_{\mathrm{df}}$, but rather to see how the model predictions are affected by various physical processes. This will tell us which process dominates the predicted $T_{\mathrm{df}}$ and how to interpret the discrepancies among the previous studies. Our model is based on Taylor & Babul (2001) and Zentner & Bullock (2003), but with a few modifications. The paper is organized as follows. In Section 2, we review the previous results. We introduce our model in Section 3, and compare our model predictions with previous works in Section 4. We briefly summarize and conclude in Section 5.

## 2 PREVIOUS RESULTS

### 2.1 Set Up of Initial Conditions

The first step in modeling the evolution of a satellite is to set its initial conditions, including the orbital energy, angular momentum and initial position. The satellite is assumed to start its orbit at the virial radius, $R_{\mathrm{vir}}$, from the host halo. It has an initial orbital energy equal to that of a circular orbit of radius $\eta R_{\mathrm{vir}}$, and the initial specific angular momentum of the satellite is parameterized as $j(0) = \varepsilon j_{\mathrm{c}}$, where $j_{\mathrm{c}}$ is the specific angular momentum of the circular orbit mentioned above and $\varepsilon$ is the orbital circularity (note that $0 \leq \varepsilon \leq 1$). In the following, we use $R_{\mathrm{m}}$ to denote the initial mass ratio between the host and satellite halo, i.e. $R_{\mathrm{m}} = M_{\mathrm{h}}(0)/M_{\mathrm{s}}(0)$.

### 2.2 Previous Results

Here we briefly review the previous studies on $T_{\mathrm{df}}$ from analytical models or $N$-body simulations. Using Chandrasekhar's formula, BT87 derived an expression of $T_{\mathrm{df}}$ for a satellite starting with a circular orbit in an isothermal distributed host halo as

$$T_{\mathrm{df,BT87}} = \frac{1.17}{\ln \Lambda} R_{\mathrm{m}} \tau_{\mathrm{dyn}}, \tag{1}$$

where $\tau_{\mathrm{dyn}}$ is the dynamical time $R_{\mathrm{vir}}/V_{\mathrm{vir}}$, and $\ln \Lambda$ is the Coulomb logarithm.

Taking into account the dependence on the orbital circularity, LC93 obtained that

$$T_{\mathrm{df,LC93}} = \frac{\varepsilon^{0.78}}{0.855} \frac{R_{\mathrm{m}}}{\ln \Lambda} \eta^2 \tau_{\mathrm{dyn}}. \tag{2}$$

Note that in the above two equations, the satellite is treated as a rigid object without mass loss.

With the help of $N$-body simulations, C99 derived $T_{\mathrm{df}}$ for an amorphous satellite to be

$$T_{\mathrm{df,C99}} = 1.2\varepsilon^{0.4} \frac{R_{\mathrm{m}}}{f_m \ln \Lambda} \eta^2 \tau_{\mathrm{dyn}}, \tag{3}$$

where $f_m$ refers to the remaining fraction of satellite mass due to tidal stripping. Note that C99 only considers minor mergers. It is difficult to use this formula as the $T_{\mathrm{df}}$ depends on the presumed value for $f_m$.

Using a semi-analytical model, T03 derived their fitting formulas for $T_{\mathrm{df}}$ and they were updated by Monaco et al. (2007). Their model has incorporated the effect of tides, but they ignored this effect for large satellites (with mass $R_{\mathrm{m}}^{-1} > 0.1$). Here we omit the complex formula of T03.

Using smoothed-particle hydrodynamical simulations with gas cooling and star formation in a cosmological context, J08 fitted their results with $T_{\mathrm{df}}$ as

$$T_{\mathrm{df, J08}} = \frac{0.9\varepsilon^{0.47} + 0.6}{0.855} \frac{R_{\mathrm{m}}}{\ln(1 + R_{\mathrm{m}})} \sqrt{\eta} \tau_{\mathrm{dyn}}. \tag{4}$$

BK08 considered controlled $N$-body simulations for two halo mergers. They gave the fitting formula of $T_{\mathrm{df}}$ as

$$T_{\mathrm{df, BK08}} = 0.216\mathrm{e}^{1.9\varepsilon} \frac{R_{\mathrm{m}}^{1.3}}{\ln(1 + R_{\mathrm{m}})} \eta \tau_{\mathrm{dyn}}. \tag{5}$$

In Figure 1, we show $T_{\mathrm{df}}$ as a function of satellite mass and orbital circularity[2] predicted by LC93, T03, J08 and BK08. For a full comparison with other results, we choose $\ln \Lambda = \ln(1 + R_{\mathrm{m}})$ in the formula of LC93. It can be seen that all results show a clear trend that $T_{\mathrm{df}}$ decreases with increasing satellite mass, but $T_{\mathrm{df}}$ increases with orbital angular momentum and energy. However, the discrepancies among different studies are still remarkable. For example, the results of BK08 and J08 are longer than those of T03 and LC93. T03 agrees well with LC93 for large satellites ($R_{\mathrm{m}}^{-1} > 0.1$), but disagrees for small satellites. The results of BK08 exhibit a steeper dependence on $\varepsilon$ than other results.

## 3 MODELING A SINKING SATELLITE

This section describes the dynamical evolution of a satellite based on the model of Taylor & Babul (2001); Zentner & Bullock (2003). In Section 3.1, we introduce the model of the mass distribution of a dark matter halo. Then we describe the physical processes governing the orbital and mass evolution of the satellite. These processes can be independently implemented into the model, which allows us to investigate the effect of any specific process by tuning its free parameter.

### 3.1 Halo Properties

The dark matter halo is a gravitational self-bound system. We express the size of the halo in terms of its virial mass $M_{\mathrm{vir}}$ and virial radius $R_{\mathrm{vir}}$, which is defined as the radius within which the mean mass density of the halo is 200 times the critical density ($\rho_c$) of the universe at $z = 0$ (e.g., Mo et

---

[2] Throughout this paper, we keep the orbital energy fixed at $\eta = 1.0$ to reduce the number of free model parameters.
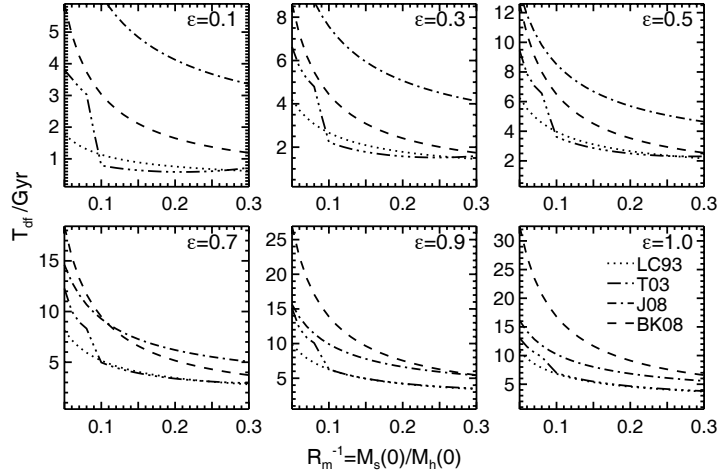
**Fig. 1** Dynamical friction timescale of a sinking satellite predicted by the formulas of Lacey & Cole (1993, LC93), Taffoni et al. (2003, T03), Boylan-Kolchin et al. (2008, BK08) and Jiang et al. (2008, J08). The six panels show the dependence on the orbital circularity $\varepsilon$, and each panel shows the dependence on the initial mass ratio between the satellite and host halo. In the results of LC93, we adopt $\ln \Lambda = \ln(1 + R_{\mathrm{m}})$, as used by T03, BK08 and J08. In all cases, $\eta = 1.0$.

al. 1998). The Hubble constant is adopted to be $H_0 = 100 \, h \, \mathrm{km \, s^{-1} \, Mpc^{-1}}$ with $h = 0.7$ (BK08). The dynamical timescale can be described as

$$\tau_{\mathrm{dyn}} = \frac{R_{\mathrm{vir}}}{V_{\mathrm{vir}}} = \left( \frac{R_{\mathrm{vir}}^3}{G M_{\mathrm{vir}}} \right)^{1/2} = 0.1 H_0^{-1} \simeq 1.40 \, \mathrm{Gyr}, \tag{6}$$

where $V_{\mathrm{vir}}$ is the virial velocity of a halo.

For simplicity, the dark matter halo is usually treated as a spherically symmetric system, and a simple formalism for the halo density profile is the profile of a singular isothermal sphere (hereafter, ISO profile), which can be described by (e.g., Mo et al. 1998)

$$\rho(r) = \frac{V_{\mathrm{vir}}^2}{4\pi G r^2}, \tag{7}$$

and

$$M(< r) = \frac{V_{\mathrm{vir}}^2}{G} r. \tag{8}$$

As measured by $N$-body simulations, the halo density profile can be well described by the NFW profile (Navarro et al. 1997)

$$\rho(r) = \frac{\delta_0 \rho_c}{(r/r_{\mathrm{s}})(1 + r/r_{\mathrm{s}})^2} , \tag{9}$$

with $r_{\mathrm{s}}$ the scale radius, and $\delta_0$ the characteristic overdensity. From the definition of virial radius, we can find the characteristic overdensity of $\delta_0 = 200 c^3 / [3g(c)]$, where $c = R_{\mathrm{vir}}/r_{\mathrm{s}}$ is the halo concentration parameter, and $g(x) = \ln(1 + x) - x/(1 + x)$. For the NFW profile, the halo mass enclosed by radius $r$ is

$$M(< r) = M_{\mathrm{vir}} \frac{g(r/r_{\mathrm{s}})}{g(c)} . \tag{10}$$

The halo concentration is tightly correlated to its mass, and we use the median relation of $c \sim M$ as measured by Neto et al. (2007)

$$c(M) = 4.67 \left( \frac{M}{10^{14}h^{-1}M_\odot} \right)^{-0.11} . \tag{11}$$

Note that there are still existing debates regarding the inner shape of the NFW profile (e.g., Fukushige & Makino 2001; Navarro et al. 2004; Stoehr 2006; Springel et al. 2008). Varying the shape of the NFW profile or using other halo profiles [e.g., ISO profile; Hernquist profile (Hernquist 1990)] may derive a different $T_{df}$. However, the simulation of BK08 indicated that using a different halo profile led to a change in $T_{df}$ of only $5\%$ (see BK08 for more details).

Except for Section 4.1, where the ISO profile is adopted to compare the model predictions with the analytical results of LC93, we use the NFW profile from other studies in this paper. When the tidal effects are considered, the satellite halo has an NFW profile at the time of entering ($t = 0$), and this profile is subsequently modified due to tidal heating, as described in Section 3.4.

In our studies, we select the host halo mass to be $10^{12}M_\odot$, which is the typical mass used to derive the $T_{df}$ (BK08, J08, C99). We have also tested that the predicted $T_{df}$ has a negligible effect on the host halo mass once the mass ratio $R_m$ is fixed.

## 3.2 Dynamical Friction

The satellite will sink into the halo center due to dynamical friction force which is caused by the gravitational interactions between the satellite and the background 'field' particles that make up the host halo (for a complete description, see BT87). This effect was first discussed by Chandrasekhar (1943), and the force generated by the field particles is known as the Chandrasekhar dynamical friction. By assuming that the field particles locally follow a Maxwellian velocity distribution, BT87 gave the formula of dynamical friction to be

$$\boldsymbol{F}_{df} = -4\pi G^2 M_s^2 \ln \Lambda \, \rho(r) \left[ \mathrm{erf}(X) - \frac{2X}{\sqrt{\pi}} e^{-X^2} \right] \frac{\boldsymbol{v}_{orb}}{v_{orb}^3} , \tag{12}$$

where $v_{orb}$ is the orbital velocity of the satellite, and $X = v_{orb}/[\sqrt{2}\sigma(r)]$ with $\sigma(r)$ the local, one-dimensional velocity dispersion of the host halo at radius $r$, which can be solved from the Jeans equation (BT87, Cole & Lacey 1996). For the ISO profile, $\sigma(r) \equiv V_{vir}/\sqrt{2}$; for the NFW profile, we use the fitting formula of $\sigma(r)$ from Zentner & Bullock (2003). We choose the Coulomb logarithm $\ln \Lambda = \ln(1 + R_m)$, as used by T03, J08 and BK08.

Equation (12) was derived with the idealized assumption that the velocity distribution of dark matter particles is Maxwellian and isotropic. Although there are debates about whether this assumption is reasonable (e.g., Manrique et al. 2003; Williams et al. 2004; Salvador-Solé et al. 2005; Bellovary et al. 2008), in this paper, we follow most authors (e.g., LC93; C99; T03; Zentener & Bullock 2003; Fellhauer & Lin 2007; BK08) and adopt the Maxwellian, isotropic velocity distribution. There are also simulations showing that this assumption is a good approximation (e.g., Cole & Lacey 1996; Sheth 1996; Seto & Yokoyama 1998; Kang et al. 2002; Hayashi et al. 2003).

## 3.3 Tidal Mass Stripping

For an amorphous satellite, the tidal force from the host halo will strip its mass. The tidal radius, $r_t$, is the distance from the center of the satellite to the radius where the external differential force from the host halo exceeds the binding force of the satellite. The tidal radius can simply be solved from the following equation (von Hoerner 1957; King 1962; Taylor & Babul 2001):

$$r_t^3 = \frac{GM_s(< r_t)}{\omega^2 + G\left[2M_h(< r)/r^3 - 4\pi\rho_h(r)\right]} , \tag{13}$$

with $\omega$ being the angular speed of the satellite and $\rho_{\mathrm{h}}(r)$ the density profile of the host halo. The mass outside $r_{\mathrm{t}}$ becomes unbound and is gradually stripped. Taylor & Babul (2001) suggested the unbound mass is stripped at the rate

$$\frac{\mathrm{d}M_{\mathrm{s}}}{\mathrm{d}t} = -\frac{M_{\mathrm{s}}(> r_{\mathrm{t}})}{T_{\mathrm{orb}}} , \tag{14}$$

with $T_{\mathrm{orb}}$ the instantaneous orbital period (i.e., $T_{\mathrm{orb}} = 2\pi/\omega$), which is assumed to be the mass stripping timescale.

There are some uncertainties in the above mechanisms of mass stripping. (i) The tidal radius cannot be characterized by a single radius, since the zero-velocity surface (the surface defined by the tidal radius, see BT87) is not spherical. (ii) The perturbation of particles within the satellite may lead to scatter in $\omega$, and the zero-velocity surface is actually a shell of 'non-zero' thickness; this effect is ignored in Equation (13). So the solution of Equation (13) is only an approximation for the tidal radius. (iii) The stripped mass from a satellite still remains in the vicinity of the satellite, and the interaction between the stripped and unstripped mass will perturb the satellite's orbit and affect the mass loss (e.g., Fellhauer & Lin 2007).

Owing to these uncertainties, numerical simulations have generated a debate on how fast the unbound mass is stripped from the satellite. Zentner et al. (2005) and Diemand et al. (2007) found a stripping timescale 3.5 and 6 times shorter than $T_{\mathrm{orb}}$, respectively. It was also pointed out that the stripping timescale is dependent on the satellite's internal structures (Kazantzidis et al. 2004; Kampakoglou & Benson 2007). In general, the mass loss rate can be described using a free parameter $\alpha$ as

$$\frac{\mathrm{d}M_{\mathrm{s}}}{\mathrm{d}t} = -\alpha\frac{M_{\mathrm{s}}(> r_{\mathrm{t}})}{T_{\mathrm{orb}}} , \tag{15}$$

where $\alpha$ describes the efficiency of tidal stripping. In Section 4.2, we will show how $T_{\mathrm{df}}$ depends on $\alpha$.

### 3.4 Tidal Heating

During the pericentric passage of the satellite's orbit, the gravitational field changes rapidly, and this induces a gravitational shock that can add energy to the satellite (e.g., Gnedin & Ostriker 1997, 1999). This effect is called tidal heating. It has been found from $N$-body simulations (e.g., Hayashi et al. 2003; Kravtsov et al. 2004) that tidal heating will expand the satellite and reduce its inner mass profile. Hayashi et al. (2003) introduced a modified NFW profile to describe the density distribution of a tidally heated satellite according to

$$\rho(r) = \frac{f_t}{1 + (r/r_{\mathrm{te}})^3}\rho_{\mathrm{NFW}}(r) , \tag{16}$$

where

$$\lg f_t = -0.007 + 0.35x_m + 0.39x_m^2 + 0.23x_m^3 , \tag{17}$$

and

$$\lg \frac{r_{\mathrm{te}}}{r_{\mathrm{s}}} = 1.02 + 1.38x_m + 0.37x_m^2 . \tag{18}$$

In Equation (16), $\rho_{\mathrm{NFW}}(r)$ is the original NFW density profile of the satellite at the time it enters the larger halo ($t = 0$), $f_t$ describes the reduction in the central density of the satellite, and $r_{\mathrm{te}}$ is the 'effective' tidal radius that describes the outer cutoff imposed by the tides. In Equations (17) and (18), $x_m = \lg[M_{\mathrm{s}}(t)/M_{\mathrm{s}}(0)]$ is the logarithm of the remaining fraction of satellite mass, and $r_{\mathrm{s}}$ is the scale radius of the satellite with the NFW profile at $t = 0$. As shown by Hayashi et al. (2003), $f_t$ and $r_{\mathrm{te}}$ are well fitted by the function $x_m$. Both $f_t$ and $r_{\mathrm{te}}$ decrease with time while a satellite is losing mass.

### 3.5 Orbital Evolution

Here we explicitly present the equations to solve the orbit $[\mathbf{x}(r,\theta)]$ of the satellite under the influence of gravity and dynamical friction. The equation of motion for the satellite is given by

$$\frac{\mathrm{d}^2 \boldsymbol{x}}{\mathrm{d}t^2} = -\frac{GM_\mathrm{h}(<r)}{r^3}\,\boldsymbol{r} + \frac{\boldsymbol{F}_\mathrm{df}}{M_\mathrm{s}} \tag{19}$$

with $M_\mathrm{h}(<r)$ the mass of the host halo inside of radius $r$, and $\boldsymbol{F}_\mathrm{df}$ the dynamical friction force given by Equation (12). The orbital energy and angular momentum of the satellite will decay due to the dynamical friction since it is always opposite to the direction of motion. We define the satellite to be merged with its host's center when it loses all of its angular momentum, and $T_\mathrm{df}$ is the time interval between accretion and merger [3] (as also used by BK08). The equation of motion and Equation (15) are solved using the fifth-order Cash-Karp Runga-Kutta method, in which an adaptive step-size control is embedded.

## 4 RESULTS

### 4.1 Examination on a Rigid Satellite

First we validate our model by comparing the predicted $T_\mathrm{df}$ with the LC93 result for a rigid satellite. LC93 derived $T_\mathrm{df}$ using Equation (12) and the ISO profile for the host halo. In our model, we simply set $\alpha = 0$ to 'close' the tidal stripping and tidal heating effect, and we model the host halo with both the NFW profile and ISO profile.

In Figure 2, we show $T_\mathrm{df}$ as a function of $R_\mathrm{m}^{-1}$ and $\varepsilon$ for a rigid satellite, with $T_\mathrm{df}$ normalized to its value when $R_\mathrm{m} = 20$ and $\varepsilon = 1$, respectively. As indicated, our results in the NFW (solid line) and ISO (dashed line) models both have the same dependences as predicted by LC93. On the other hand, the amplitudes of $T_\mathrm{df}$ from the models also agree well with the results of LC93, which is demonstrated in Figure 3. The differences resulting from varying halo profiles are small and negligible, which is the same conclusion as reached by BK08.
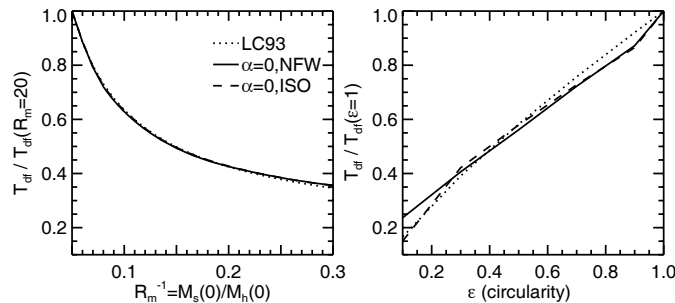


**Fig. 2** Dependence of $T_\mathrm{df}$ on satellite mass (*left panel*) and orbital circularity (*right panel*) for a rigid satellite, where $T_\mathrm{df}$ is normalized to its value when $R_\mathrm{m} = 20$ and $\varepsilon = 1$, respectively. The model with $\alpha = 0$ means that a rigid satellite is considered. The results in solid lines are computed with the NFW profile, while the dashed lines show the results with the ISO profile. Both model predictions match well with LC93's (*dotted line*).

---

[3] Some authors (e.g., Kravtsov et al. 2004; Zentner et al. 2005) define a satellite to be merged with the host halo when its distance to the host center is less than a fiducial radius. We find that different definitions have no significant effects.
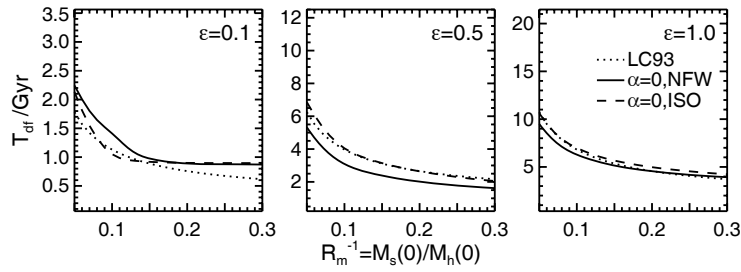
**Fig. 3** Comparison of $T_{\mathrm{df}}$ between our model ($\alpha = 0$) and LC93 (*dotted line*) for a rigid satellite. The $T_{\mathrm{df}}$ with the NFW profile (*solid line*) and ISO profile (*dashed line*) both agree well with LC93's prediction, and they agree for all orbital circularities, although only $\varepsilon$ values with $0.1, 0.5$, and $1.0$ are given here.
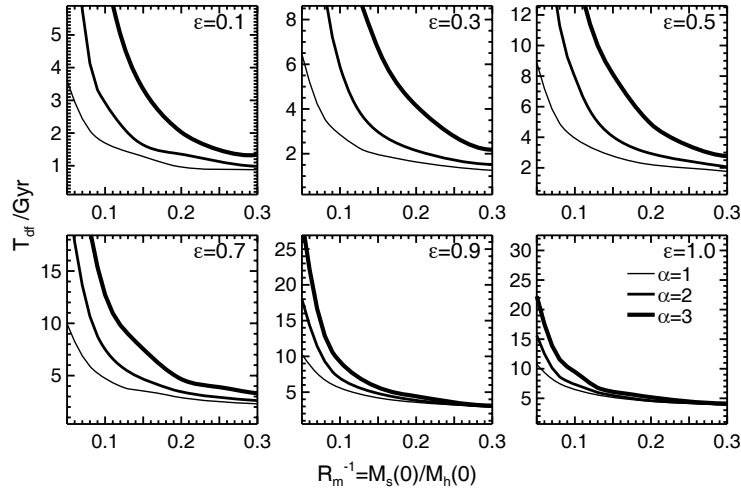


**Fig. 4** Dynamical friction timescale ($T_{\mathrm{df}}$) predicted by our model. The lines with increasing thickness show the effects of tidal stripping efficiency ($\alpha = 1, 2, 3$). The $T_{\mathrm{df}}$ is a strong function of $\alpha$.

## 4.2 Dependence on Tidal Stripping Efficiency $\alpha$

In this section, we study the effects of tidal stripping efficiency ($\alpha$). In Figure 4, we show the predicted $T_{\mathrm{df}}$ with different values of $\alpha$. A larger value of $\alpha$ corresponds to a stronger tidal field or a rapid mass loss from the satellite. The results show a remarkable trend that the $T_{\mathrm{df}}$ is increased when the tidal field becomes stronger. The reason can be seen from Figure 5 which shows the evolution of satellite mass and specific angular momentum with dependence on $\alpha$. The initial conditions are set to $R_{\mathrm{m}} = 10$, $\varepsilon = 0.5$, and $\eta = 1.0$. The left panel shows that a stronger tidal field will induce more mass loss from the satellite, and this effect is more distinct at the beginning. As seen from Equation (12), the amplitude of dynamical friction has a strong dependence on the mass of the satellite ($F_{\mathrm{df}} \propto M_s^2$). So a stronger tidal stripping will lead to a slower decay of the satellite's angular momentum and will result in a longer dynamical friction timescale, as shown in the right panel of Figure 5.
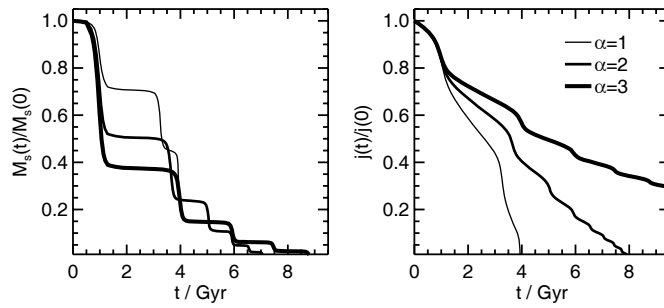
**Fig. 5** Evolution of satellite mass and specific angular momentum (both are normalized to their initial value) as a function of tidal stripping efficiency $\alpha$. The initial conditions are that $R_\mathrm{m} = 10$, $\varepsilon = 0.5$, and $\eta = 1.0$. Strong tidal effects reduce the amplitude of dynamical friction and decelerate the loss of angular momentum.
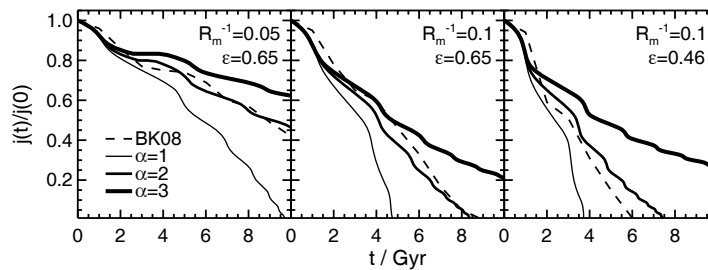


**Fig. 6** Comparison of the evolution of a satellite's specific angular momentum between our model and BK08, with three cases of initial masses and orbits as indicated. The solid lines with increasing thickness are the model results with $\alpha = 1, 2, 3$, while the dashed line is the result from fig. 1 of BK08. The tidal stripping efficiency in the simulation of BK08 should be stronger than that in a model with $\alpha = 1$.

As shown in Figure 1, the predicted $T_\mathrm{df}$ values from the previous results quantitatively disagree with each other. We believe that the main discrepancy is a result of the treatment of tidal stripping, and we discuss it in more detail in the following.

– T03 ignored the tidal effects for a massive satellite (with mass $R_\mathrm{m}^{-1} > 0.1$), and so their $T_\mathrm{df}$ values are consistent with LC93's. However, T03 predicted a longer $T_\mathrm{df}$ for a low-mass satellite which suffers from tidal stripping.

– The $T_\mathrm{df}$ values inferred by J08 and BK08 are longer than those of T03. This is because T03 adopted a tidal stripping efficiency that is different from those in $N$-body simulations. T03 also used Equation (15) to describe the mass loss, but with $\alpha = 1.0$ which is too low. As shown by Zentner et al. (2005), a higher value than $\alpha = 3.5$ is required to better fit the satellite mass function from simulations (also see Gan et al. 2010). A higher value of $\alpha$ is also favored from Figure 6 where we compare the evolution of a satellite's specific angular momentum from our model (solid lines) with the simulation results of BK08 (dashed lines). We find that $\alpha = 2$ can better match the simulation results. Thus, the lower value of $\alpha$ used by T03 explains why they obtained a lower $T_\mathrm{df}$.

– The $T_{\mathrm{df}}$ of J08 is longer than that of BK08 for an eccentric orbit (i.e., low $\varepsilon$)[4]. The simulation of J08 includes the process of gas cooling and star formation. The halo of a satellite is expected to contract in response to the cooling of gas (e.g., Gnedin et al. 2004; Abadi et al. 2010). During the pericentric passage, the satellite with halo contraction is resistant to the strong tidal field, and will survive for a longer time (e.g., Weinberg et al. 2008; Dolag et al. 2009). Instead, BK08 performs a higher resolution simulation, in which the satellite can avoid the artificial mass loss due to the numerical effects. So the satellite will deposit more mass in the eccentric orbit and will suffer stronger dynamical friction.

### 4.3 Dependence on Orbital Circularity $\varepsilon$

The previous results showed a similar dependence of $T_{\mathrm{df}}$ on the initial satellite mass, but very different dependences on the orbital circularity [Equations (2)–(5)]. For example, BK08 found an exponential dependence of $T_{\mathrm{df}}$ on the the orbital circularity, while others found a power-law dependence. Here we investigate this problem using our model with $\alpha = 1$. We compute the $T_{\mathrm{df}}$ as a function of $\varepsilon$ for a minor merger ($R_{\mathrm{m}}^{-1} = 0.05$) and a major merger ($R_{\mathrm{m}}^{-1} = 0.3$), as shown in Figure 7. We find that the dependence for the minor merger can be fitted to a power law, $T_{\mathrm{df}} \propto \varepsilon^{0.4}$, as predicted by C99 (long-dashed). For the major merger, the dependence is close to the result of BK08, who found an exponential law of $T_{\mathrm{df}} \propto \exp(1.9\varepsilon)$. It is not a surprise because C99 only considers minor mergers while BK08 has more samples for the major mergers. Thus, we argue that the dependence on orbital circularity is mainly determined by the distribution of mass ratios between the satellite and host halo.
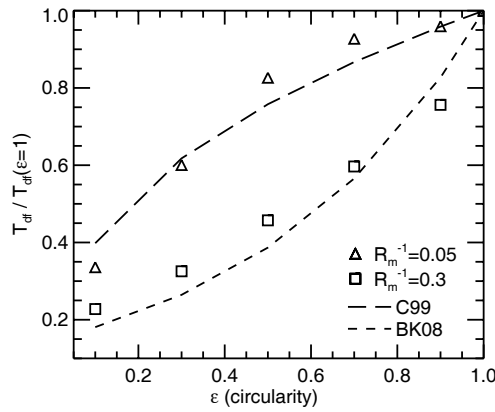


**Fig. 7** Dependence of $T_{\mathrm{df}}$ on orbital circularity for an amorphous satellite ($\alpha = 1$). For a minor merger (*triangle*), with $R_{\mathrm{m}}^{-1} = 0.05$, the result shows a power-law dependence, which is similar to that of C99 (*long-dashed line*), while for a major merger (*square*), with $R_{\mathrm{m}}^{-1} = 0.3$, it indicates an exponential dependence, which is close to that of BK08 (*short-dashed line*).

## 5 CONCLUSIONS AND DISCUSSION

In this paper, we study the dynamical friction timescale ($T_{\mathrm{df}}$) of a satellite sinking into a host halo. Previous results using analytical models or simulations generally agree that the $T_{\mathrm{df}}$ is correlated

---

[4] The results of BK08 and J08 also differ for a small satellite with large $\varepsilon$, for which the $T_{\mathrm{df}}$ values, however, are extrapolated by their formulas and exceed the Hubble time.

with the mass, orbital circularity and energy of the satellite, but disagree on the amplitude of $T_{\mathrm{df}}$ and the dependence of $T_{\mathrm{df}}$ on orbital circularity. It was unclear what contributes to these discrepancies among the different studies.

Aiming at interpreting these different dependences, we use a semi-analytical model similar to that of Taylor & Babul (2001) and Zentner & Bullock (2003) to derive the $T_{\mathrm{df}}$. Our model considers the main physical processes governing the evolution of a satellite: dynamical friction, tidal stripping, tidal heating and merging. All these processes are independently described by free parameters, and it allows us to investigate the dependence of $T_{\mathrm{df}}$ on any process.

First, we apply our model to a rigid satellite by 'turning off' the tidal stripping and tidal heating (i.e. $\alpha = 0$). The model predictions agree well with LC93's result of the amplitude of $T_{\mathrm{df}}$ and its dependences on satellite mass and orbital circularity. Then we study the dependence of $T_{\mathrm{df}}$ on the tidal stripping efficiency. We find that $T_{\mathrm{df}}$ depends strongly on $\alpha$, with the trend that $T_{\mathrm{df}}$ increases with increasing $\alpha$. A higher $\alpha$ leads to rapid loss of mass from the satellite, then decreases the dynamical friction force. Thus this results in a slower decay of angular momentum and a longer $T_{\mathrm{df}}$. We believe that the main reason for the diversity of the previous results is the treatment of tidal stripping.

We also study the dependence of $T_{\mathrm{df}}$ on orbital circularity ($\varepsilon$). We find that for low mass-ratio mergers ($M_{\mathrm{s}}/M_{\mathrm{h}} < 0.1$), $T_{\mathrm{df}}$ is a power law of orbital circularity, but for massive mergers ($M_{\mathrm{s}}/M_{\mathrm{h}} > 0.1$), the dependence of $T_{\mathrm{df}}$ on orbital circularity is exponential. Thus, we argue that the dependence on $\varepsilon$ obtained by different studies is determined by their samples, in which the mass ratio between the satellite and host halo is crucial.

In this paper, we do not model the effects of baryons, since it is difficult to include in the physical processes governing galaxy formation, and it is still not clear how the dark matter halo will respond to the baryon at the host halo center.

The major effect of the baryons is to modify the density profile of the dark matter halo. There are still debates about how the baryon will change the central concentration of the halo. Some found that central density increases (e.g., Blumenthal et al. 1986; Gnedin et al. 2004), but others disagreed with this assertion. Gnedin et al. (2004) found that the halo will become more concentrated as baryons condense in the radiative cooling, and the contraction of the halo depends on the amount of baryons. Moreover, Abadi et al. (2010) found that the response of halo contraction depends not only on how much baryon mass has been deposited by the halo, but also on the mode of its deposition (also see Tissera et al. 2010). They showed that strong feedback by supernovae can significantly decrease the central density of the halo (also see Pedrosa et al. 2009; Governato et al. 2010). The variation of $T_{\mathrm{df}}$ is about $20\%$ when $c_{\mathrm{sat}}/c_{\mathrm{host}}$ changes between $1$ and $2$ (T03; BK08).

There are also some studies showing that the dark matter haloes have constant density cores (e.g., Gilmore et al. 2007; de Blok et al. 2008; Kuzio de Naray et al. 2009; Gebhardt & Thomas 2009; Hernandez & Lee 2010), which can significantly suppress the effect of dynamical friction (e.g., Sánchez-Salcedo et al. 2006; Inoue 2009). However, the typical size of the constant density core in the dark matter halo is usually less than 1 kpc (e.g., de Blok et al. 2008). The effect of the constant density core may be remarkable for the evolution of globular clusters in a dwarf galaxy (e.g., Sánchez-Salcedo et al. 2006), but not for the evolution of a satellite halo in a Milky-Way sized halo.

# References

Abadi, M. G., Navarro, J. F., Fardal, M., Babul, A., & Steinmetz, M. 2010, MNRAS, 847

Bellovary, J. M., Dalcanton, J. J., Babul, A., Quinn, T. R., Maas, R. W., Austin, C. G., Williams, L. L. R., & Barnes, E. I. 2008, ApJ, 685, 739

Benson, A. J., Lacey, C. G., Baugh, C. M., Cole, S., & Frenk, C. S. 2002, MNRAS, 333, 156

Benson, A. J., Lacey, C. G., Frenk, C. S., Baugh, C. M., & Cole, S. 2004, MNRAS, 351, 1215

Binney, J., & Tremaine, S. 1987, Galactic Dynamics (Princeton: Princeton University Press), 747 (BT87)

Blumenthal, G. R., Faber, S. M., Flores, R., & Primack, J. R. 1986, ApJ, 301, 27

Boylan-Kolchin, M., Ma, C.-P., & Quataert, E. 2008, MNRAS, 383, 93 (BK08)

Chandrasekhar, S. 1943, ApJ, 97, 255

Cole, S., & Lacey, C. 1996, MNRAS, 281, 716

Cole, S., Lacey, C. G., Baugh, C. M., & Frenk, C. S. 2000, MNRAS, 319, 168

Colpi, M., Mayer, L., & Governato, F. 1999, ApJ, 525, 720 (C99)

de Blok, W. J. G., Walter, F., Brinks, E., Trachternach, C., Oh, S.-H., & Kennicutt, R. C. 2008, AJ, 136, 2648

Diemand, J., Kuhlen, M., & Madau, P. 2007, ApJ, 667, 859

Dolag, K., Borgani, S., Murante, G., & Springel, V. 2009, MNRAS, 399, 497

Fellhauer, M., & Lin, D. N. C. 2007, MNRAS, 375, 604

Fukushige, T., & Makino, J. 2001, ApJ, 557, 533

Gan, J., Kang, X., van den Bosch, F. C., & Hou, J. 2010 (arXiv:1007.0023)

Gebhardt, K., & Thomas, J. 2009, ApJ, 700, 1690

Gilmore, G., Wilkinson, M. I., Wyse, R. F. G., Kleyna, J. T., Koch, A., Evans, N. W., & Grebel, E. K. 2007, ApJ, 663, 948

Gnedin, O. Y., & Ostriker, J. P. 1997, ApJ, 474, 223

Gnedin, O. Y., & Ostriker, J. P. 1999, ApJ, 513, 626

Gnedin, O. Y., Kravtsov, A. V., Klypin, A. A., & Nagai, D. 2004, ApJ, 616, 16

Governato, F., et al. 2010, Nature, 463, 203

Hayashi, E., Navarro, J. F., Taylor, J. E., Stadel, J., & Quinn, T. 2003, ApJ, 584, 541

Hernandez, X., & Lee, W. H. 2010, MNRAS, 404, L6

Hernquist, L. 1990, ApJ, 356, 359

Inoue, S. 2009, MNRAS, 397, 709

Jiang, C. Y., Jing, Y. P., Faltenbacher, A., Lin, W. P., & Li, C. 2008, ApJ, 675, 1095 (J08)

Kampakoglou, M., & Benson, A. J. 2007, MNRAS, 374, 775

Kang, X., Jing, Y. P., Mo, H. J., & Börner, G. 2002, MNRAS, 336, 892

Kang, X., Jing, Y. P., Mo, H. J., & Börner, G. 2005, ApJ, 631, 21

Kauffmann, G., Colberg, J. M., Diaferio, A., & White, S. D. M. 1999, MNRAS, 303, 188

Kazantzidis, S., Mayer, L., Mastropietro, C., Diemand, J., Stadel, J., & Moore, B. 2004, ApJ, 608, 663

Kazantzidis, S., Bullock, J. S., Zentner, A. R., Kravtsov, A. V., & Moustakas, L. A. 2008, ApJ, 688, 254

King, I. 1962, AJ, 67, 471

Kravtsov, A. V., Gnedin, O. Y., & Klypin, A. A. 2004, ApJ, 609, 482

Kuzio de Naray, R., McGaugh, S. S., & Mihos, J. C. 2009, ApJ, 692, 1321

Lacey, C., & Cole, S. 1993, MNRAS, 262, 627 (LC93)

Manrique, A., Raig, A., Salvador-Solé, E., Sanchis, T., & Solanes, J. M. 2003, ApJ, 593, 26

Mo, H. J., Mao, S., & White, S. D. M. 1998, MNRAS, 295, 319

Monaco, P., Fontanot, F., & Taffoni, G. 2007, MNRAS, 375, 1189

Navarro, J. F., Frenk, C. S., & White, S. D. M. 1995, MNRAS, 275, 56

Navarro, J. F., Frenk, C. S., & White, S. D. M. 1997, ApJ, 490, 493

Navarro, J. F., et al. 2004, MNRAS, 349, 1039

Neistein, E., & Weinmann, S. M. 2010, MNRAS, 405, 2717

Neto, A. F., et al. 2007, MNRAS, 381, 1450

Pedrosa, S., Tissera, P. B., & Scannapieco, C. 2009, MNRAS, 395, L57

Salvador-Solé, E., Manrique, A., & Solanes, J. M. 2005, MNRAS, 358, 901

Sánchez-Salcedo, F. J., Reyes-Iturbide, J., & Hernandez, X. 2006, MNRAS, 370, 1829

Seto, N., & Yokoyama, J. 1998, ApJ, 492, 421

Sheth, R. K. 1996, MNRAS, 279, 1310

Somerville, R. S., & Primack, J. R. 1999, MNRAS, 310, 1087

Springel, V., White, S. D. M., Tormen, G., & Kauffmann, G. 2001, MNRAS, 328, 726

Springel, V., et al. 2008, MNRAS, 391, 1685

Stoehr, F. 2006, MNRAS, 365, 147

Taffoni, G., Mayer, L., Colpi, M., & Governato, F. 2003, MNRAS, 341, 434 (T03)

Taylor, J. E., & Babul, A. 2001, ApJ, 559, 716

Tissera, P. B., White, S. D. M., Pedrosa, S., & Scannapieco, C. 2010, MNRAS, 786

von Hoerner, S. 1957, ApJ, 125, 451

Weinberg, D. H., Colombi, S., Davé, R., & Katz, N. 2008, ApJ, 678, 6

Williams, L. L. R., Babul, A., & Dalcanton, J. J. 2004, ApJ, 604, 18

Zentner, A. R., & Bullock, J. S. 2003, ApJ, 598, 49

Zentner, A. R., Berlind, A. A., Bullock, J. S., Kravtsov, A. V., & Wechsler, R. H. 2005, ApJ, 624, 505